Vergleichende Untersuchungen der Rissausbreitung in Beton mit Schallemission und digitaler Bildkorrelation

Comparative Studies of Crack Propagation in Concrete using Acoustic Emission and Digital Image Correlation

Gregor FISCHER [1], Jürgen BOHSE [2]
[1] Technical University of Denmark, Kgs. Lyngby, Dänemark
[2] Berlin, Deutschland *)

Abstract. The formation of cracks and the development of the fracture process zone (FPZ) have typically been documented by Acoustic Emission (AE) methods and important conclusions regarding the nature of the FPZ and the propagation mechanisms of concrete have been drawn to form the basis of current fracture models for concrete.

The study presented in this paper focuses on Mode I cracking of ultra-high performance concrete (UHPC) and fibre-reinforced concrete material (UHPC/steel fibres) using compact tension specimens. It compares the results of AE measurements to those obtained from documenting the cracking process by Digital Image Correlation (DIC). The findings from this comparison show that different types of AE signals from deformation mechanisms of different nature occur in distinct regions of the entire cracking process, i.e. ahead of the crack tip, at the crack tip and in the wake of the crack due to the increasing separation of the crack faces and further opening of the crack. The DIC measurements indicate that crack initiation occurs with locally corresponding AE signals and furthermore suggest a continuously connected path of the fracture process zone from initiation at the crack tip to the stress free region in the wake of the crack. Based on these comparative measurements the study shows that crack formation in UHPC is initiated by an individual, sharp micro-crack rather than by a region of diffuse micro-cracking ahead of the eventual crack tip. Later on a single macro-crack propagates. Fibrous filling of UHPC yields widespread AE sources around all crack paths and crack branches originating from the main macro-crack. AE signals detected using wideband sensors exhibit quite different characteristics in time (waveform) and frequency (bandwidth) domain. In addition to three types of AE signals from different source mechanisms in concrete already described [13] a fourth type of signals in fibre-reinforced concrete probably related to the process of fibre pull-out is detected.

*) im Ruhestand (bis Sept. 2014: Bundesanstalt für Materialforschung und -prüfung, Berlin)

1. Introduction

Crack formation and propagation in concrete is governed by formation of a crack pattern and path due to the heterogeneity of the concrete microstructure and the presence of a stress field. Crack propagation in concrete has proven to be a complex phenomenon and the mechanisms behind concrete fracture have not yet been fully understood. Concrete fracture is typically described by the concept of the fracture process zone (FPZ). The concept of the development of a FPZ is to a large extent based on acoustic emission techniques [1].

The description of concrete fracture has been repeatedly reassessed since the ground-breaking work on brittle fracture by Griffth [2]. Describing concrete fracture using linear elastic fracture mechanics is today known to be inappropriate due to the large extent of the FPZ in concrete. The problems associated with describing concrete fracture with Griffth's theory were believed to be accommodated by introducing cohesive models applied in non-linear elastic-plastic fracture mechanics, and thereby accommodating the issues associated with a large non-linear zone ahead of the crack tip [3], [4].

Although the models of Dugdale and Barenblatt still required the FPZ to be small, they provided inspiration to Hillerborg's Fictitious Crack Model [5] in which there are no restrictions to the length of the FPZ. Hillerborg's model was extended into the Crack Band Model by Bazant and Oh [6] in which the width of FPZ was accounted for. The basis of improving the fracture models of concrete has been the assumed existence and significance of the FPZ. It has been attempted by many authors to describe the FPZ and especially to determine the size of it and various measurement methods have been presented.

Today the most commonly applied method when investigating the FPZ is Acoustic Emission (AE) and the current understanding and modelling of the FPZ is mainly based on AE measurements. AE is a commonly used measurement technique for evaluation of the FPZ. There are a number of methods available for FPZ detection, but AE is described as one of the most promising methods [1]. By Otsuka and Date [7] AE is used for FPZ detection during an experiment similar to the one in the present paper. One of the advantages of AE is that cracking inside a specimen can be detected, whereas most other techniques only observe the specimen surface. However, in order to obtain reasonable accuracy the sensors must be placed in close proximity to the crack [1].

For damage classification often conventional features of AE signals or its correlation plots for identification of source mechanisms are used, e.g. [8 – 10], however, their appropriateness for a clear and reliable separation of source mechanisms has to be confirmed. Waveform features of AE signals (peak amplitude, rise time, duration) from the same source depend on material and wave propagation effects (attenuation and dispersion) [11]. The peak amplitude can be distance corrected and, hence, related to the source amplitude but amplitude distributions from different mechanisms often overlap each other. Other derived features like the RA (= rise time / peak amplitude) value partially are not really meaningful because different source mechanisms can originate signals where rise times and peak amplitudes are correlated in a different way. Thereby damage mechanisms cannot be clearly separated.

The combination of Digital Image Correlation (DIC) and AE measurements for damage monitoring and characterization of fibre-reinforced mortar was applied [12].

In earlier paper [13] studies of the fracture process and arising micro-failure mechanisms in unreinforced concrete using DIC alongside with AE technique were demonstrated. The objective of experiments published in this article is to perform similar studies of the fracture behaviour of ultra-high performance concrete (UHPC) compared to fibre-reinforced concrete (UHPC/steel fibres) to investigate the effect of fibrous filler on the FPZ and resulting fracture toughness as well. From the analysis of AE signals different mechanisms of micro-failure are derived.

2. Experimental setup

2.1 Materials, geometry and loading of specimens

The specimens consist of a pure ultra-high strength mortar (UHPC) or reinforced with smooth steel fibres (UHPC/steel fibres), which have been cast individually in horizontal orientation as plates with dimensions of 500mm by 500mm by 25mm thickness. The specimens were cast with a recess of width 100mm and depth 50mm (Figure 1).

To enable the investigation of a "simple" crack pattern it is attempted to prepare a test specimen that will develop one isolated crack that propagates in small increments. A notch of length 150mm was cut by saw blade from the recess towards the centre of the specimen to control the direction of the crack and to be able to anticipate the origin and the path of the crack. The single notch compact tension (CT) specimen is shown in Fig. 1. The DIC observation area is indicated by the shaded rectangle region and the six AE sensors attached around. Loading of the notch faces causes crack initiation at the tip of the notch and further crack propagation under crack opening Mode I.

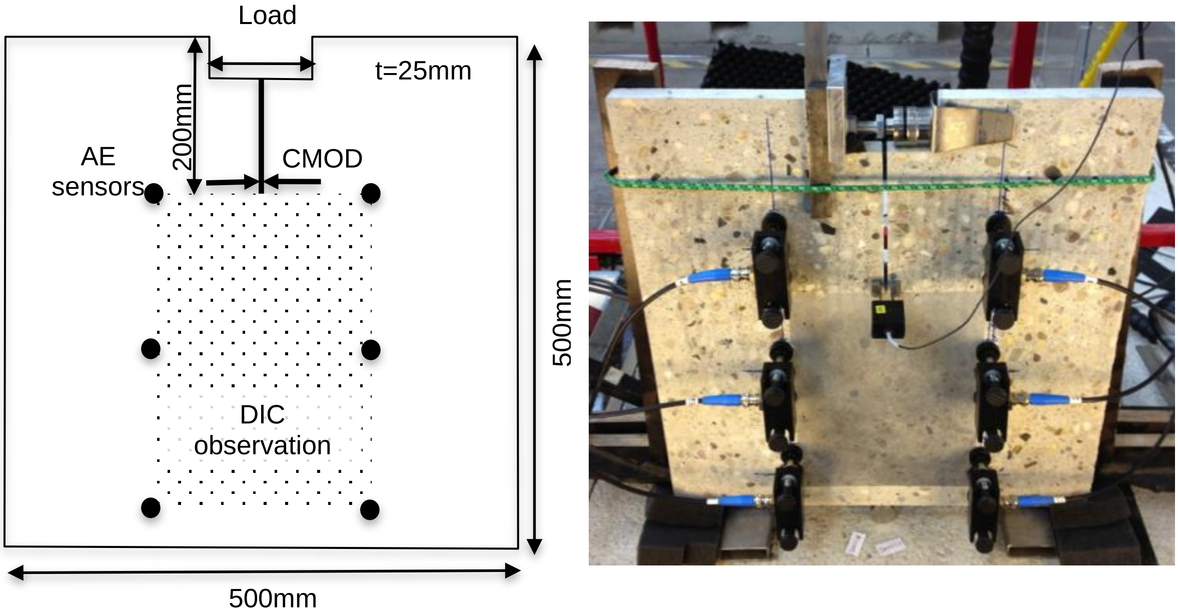

Figure 1. Experimental setup schematically (left) and specimen with fixed AE sensors, crack opening measurement (CMOD) and loading device (right).

The loading was applied using a manually operated screw mechanism to ensure a stable propagation of the crack by incremental increase in CMOD on average at 1.5μm per second. Images were taken at intervals of 5s and AE signals were permanently recorded. Each stage of crack opening is to be observed by DIC, investigating if additional information on crack growth mechanisms can be obtained by DIC and/or by simultaneously performed AE measurements.

Examples of measured load-CMOD curves from unmodified and fibre-reinforced UHPC specimens using a conventional clip gage and a load cell are shown in Figure 2.

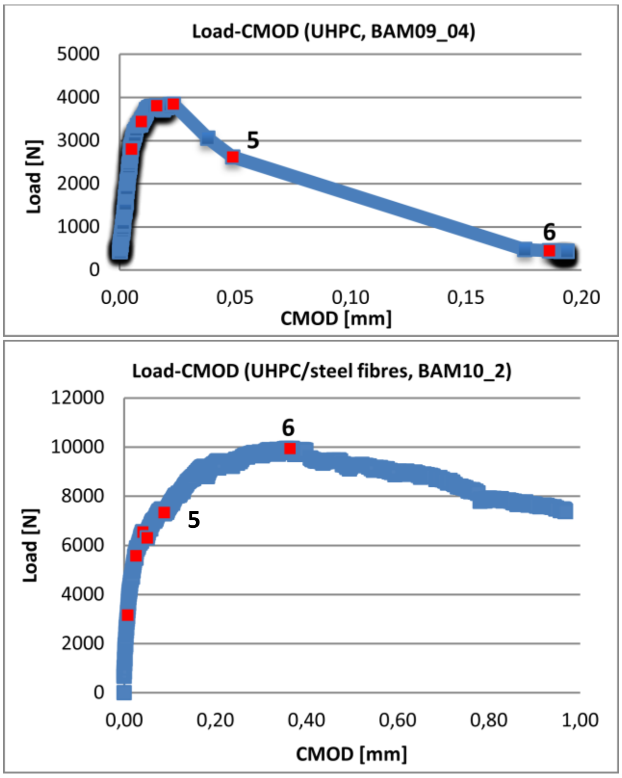

Figure 2. Load-CMOD relationship obtained for UHPC specimen BAM09_04 (top) and UHPC/steel fibres specimen BAM10_02 (bottom) with marked stages 5 and 6 of crack propagation

2.2 Digital Image Correlation (DIC) and Acoustic Emission (AE) measurements

Photos are analysed using DIC with the software Aramis (GOM Braunschweig, Germany). Series of images are processed and the displacement field of each stage is computed with reference to stage 0 which is the undeformed stage. The software creates a grid of rectangular shaped facets and computes the information in the four corners of each facet. Throughout this study the chosen facet size is 15 pixels by 15 pixels with an overlap of 2 pixels which in this study corresponds to facets of approximately 200-300µm.

Aramis computes the displacement field by finding the same points in each image of the series, thus it must be able to recognize different points on the surface. In general a concrete surface may be too uniform for the software to distinguish between points on the surface. Typically surface contrast is applied by spray painting the surface slightly with two high contrast colours, e.g. white and black.

AE measurements were performed using a MISTRAS system and six wideband sensors type PAC-WD in a rectangular sensor array surrounding the DIC observation area to locate source events by 2D Planar (XY) location type. Parameters of AE measuring setup were: pre-amp. 40dB, detection threshold 34dB_{AE}, analogue filter 20kHz...2MHz, sample rate 5MSPS and length 3k with 20µs pre-trigger for waveform recording. The maximum distance of AE sources to the nearest AE sensor was 85mm. A high attenuation (20...30dB) in this near-field distance is observed. Measured attenuation curves were used for recalculation of signal peak amplitudes at location of sources. Wave propagation of that distance causes some loss of signal power in the frequency range below 600kHz only.

Examples for similar stages of cracking in UHPC and UHPC/steel fibre specimens using the image analysis software to visualize the deformations occurring at the specimen surface are shown in Fig. 3. Here, the blue colour indicates zero surface deformations (strain) and the changing colours of the spectrum up to red indicate areas of increasing deformations. For comparison also the results of AE source localization are demonstrated.

UHPC

UHPC/steel fibres

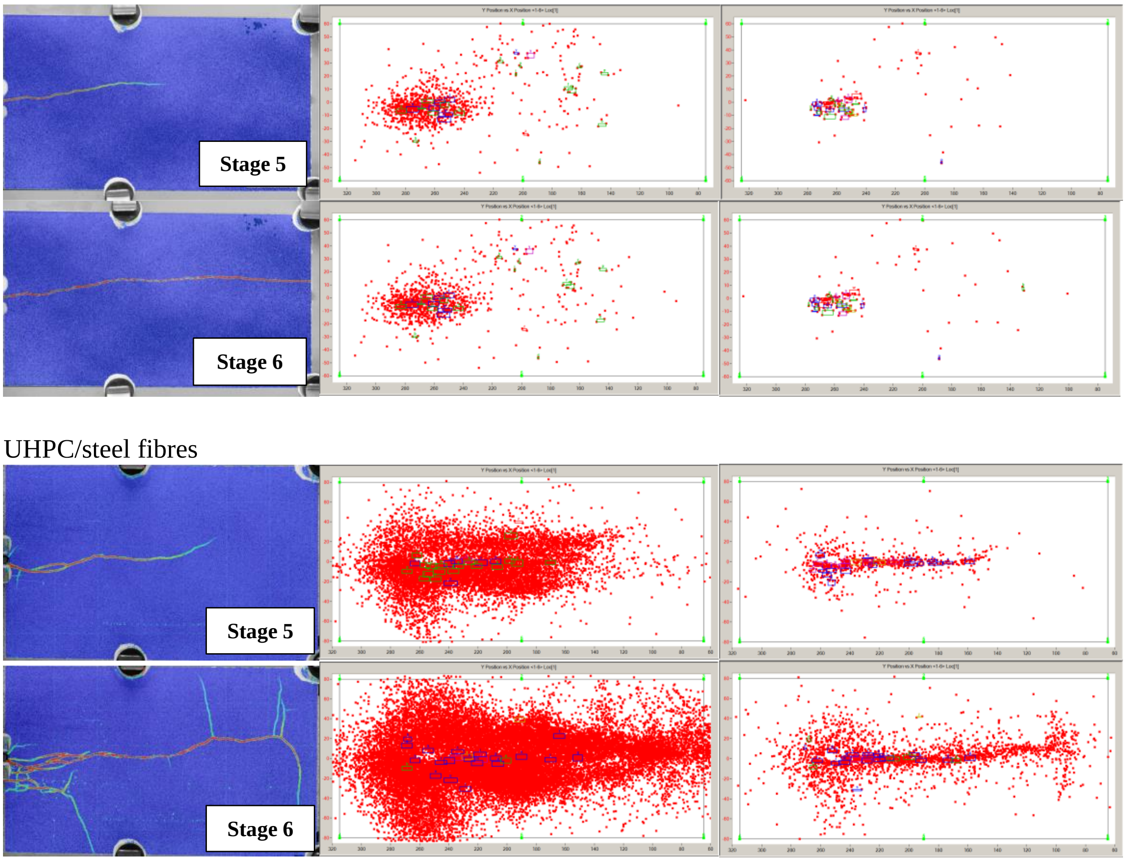

Figure 3. Crack formation in UHPC specimen BAM09_04 (top) and UHPC/steel fibres specimen BAM10_02 (bottom): Extent of cracking at stage 5 and 6 (see Fig. 2) determined by DIC of cracks (left) and located AE sources calculated using detection threshold ($34dB_{AE}$; middle) and evaluation threshold ($60dB_{AE}$; right) respectively

3. Results and Discussion

3.1 Comparison of DIC and AE results

In contrast to typical coarse concrete the morphology of UHPC is fine-grained. This yields to onset of micro-failure mechanisms and initiation of the macro-crack at higher stress levels but also to more unstable macro-crack propagation. It is apparent that cracking in the UHPC specimen occurs rather discrete and brittle by formation of a small FPZ and only one straight growing crack without signs of branching cracks.

The fibrous filler in UHPC/steel fibre material has the aim to enhance the strength in addition. However, fibre/cement interfaces are also weak points for micro-crack initiation similar to cracking along sand grain boundaries in coarse concrete but much numerous. The initiation and propagation of the macro-crack in UHPC/steel fibre specimens is connected with formation of an extended FPZ and a number of crack branches. During separation of the crack faces the mechanism of fibre pull-out can be observed, however, rupture of steel fibres can be assumed not to occur due to the high tensile strength and ductility of the fibres. Both, the large FPZ mainly caused by debonding/cracking of fibre/cement interfaces and macro-crack propagation along different crack paths under participation of fibre pull-out processes yield high energy dissipation and, hence, are reasons for the ductile fracture behaviour of fibre-reinforced UHPC.

Localized AE sources picture the contour of the FPZ and specify the different macro-crack paths. The analysis of AE results using application of the higher evaluation threshold and an energy-based clustering (open rectangles of different colours) includes AE signals of higher intensity only and, hence, sharpens the statement about main paths of crack propagation.

3.2 Analysis of AE signals

AE signals from apparently different source mechanisms were located in distinct regions but at <u>comparable source-sensor distance</u> (i.e. similar influence of attenuation and dispersion effects) before crack initiation and during crack propagation. Analysis of waveforms and frequency contents (Fig. 4) of measured AE signals result in three (UHPC) and four (UHPC/steel fibres) types/clusters respectively with quite different characteristics in both, the time and frequency domain:

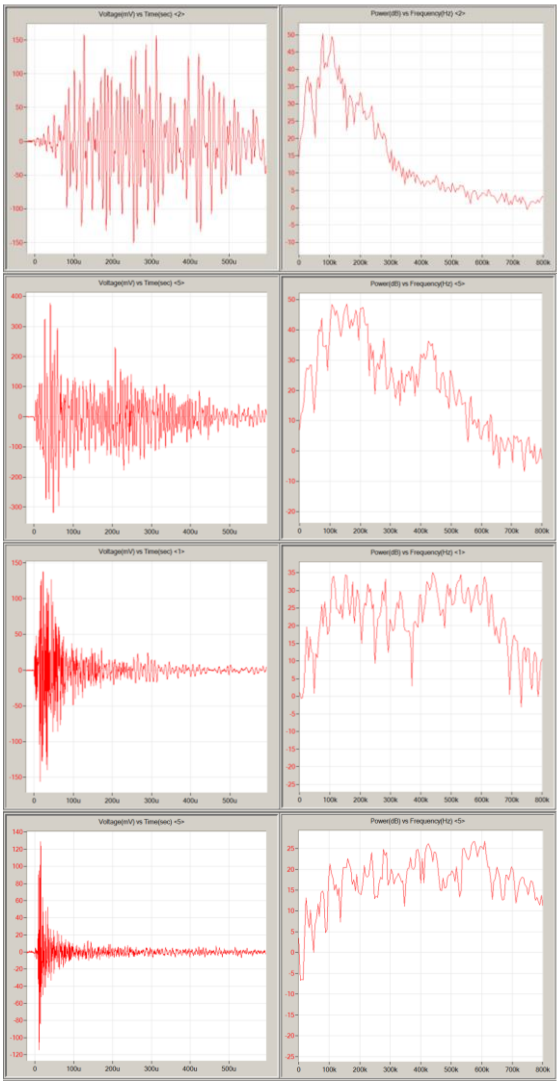

<u>*Type 1*:</u> few “continuous”-like AE signals have long duration/rise times, weighted peak-frequencies $f_{\text{weighted peak}} \approx$ 100…150kHz and source amplitudes $A_{\text{source}} \leq 95\text{dB}_{\text{AE}}$

<u>*Type 2*:</u> most measured burst-type signals are characterized by shorter duration/rise times, $f_{\text{weighted peak}} \approx$ 100…220kHz and A_{source} (UHPC) $\leq 100\text{dB}_{\text{AE}}$ / A_{source} (UHPC/steel fibres) $\leq 115\text{dB}_{\text{AE}}$

<u>*Type 3*:</u> burst-type signals that have yet shorter duration/rise times, $f_{\text{weighted peak}} \approx$ 220…350kHz but of lower source amplitudes A_{source} (UHPC) $\leq 80\text{dB}_{\text{AE}}$ / A_{source} (UHPC/steel fibres) $\leq 105\text{dB}_{\text{AE}}$

<u>*Type 4* (UHPC/steel fibres only):</u> burst-type signals that are very broadband, $f_{\text{weighted peak}} \approx$ 370…600kHz and source amplitudes $A_{\text{source}} \leq 100\text{dB}_{\text{AE}}$.

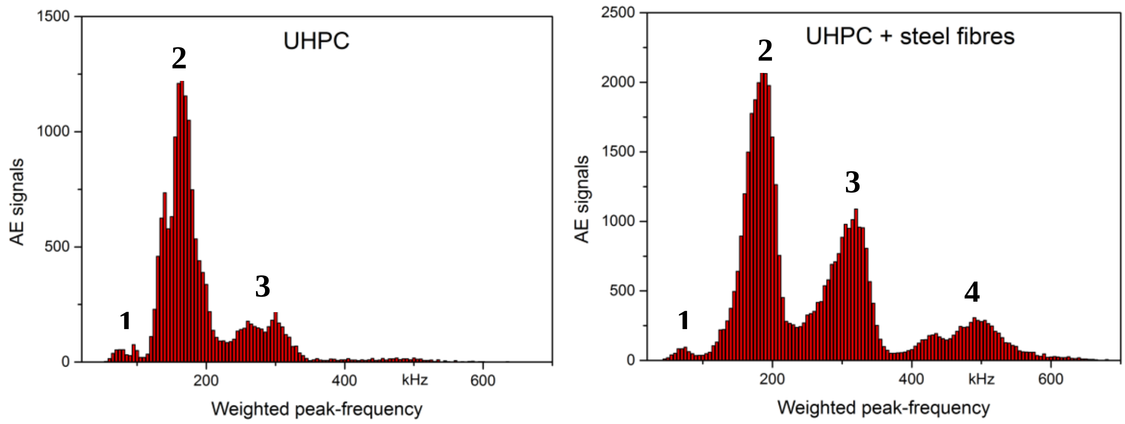

$$f_{weighted\ peak} = \sqrt{f_{peak} \cdot f_{centroid}} \qquad \text{(see [14, 15])}$$

Figure 4. Weighted peak-frequency distribution of AE signals from located events in time period up to stage 6 shown in Fig. 3

Above mentioned types of AE signals can be interpreted as follows:

Type 1: Microscopic friction-like or shear pre-damage located at the transition of the elastic region into the FPZ ahead of the macro-crack tip. Those sources mark the paths of later macro-crack propagation and occurring crack branches along weak structural regions and/or areas of particularly high stress concentrations. The real mechanism is yet unclear for the authors.

Type 2: Signals of this type arise from incremental crack growth on the microscopic level during macro-crack propagation. Thereby, measured burst signal amplitude is proportional to involved area and velocity of the micro-cracking process. The bandwidth of signal is indirect proportional to the rise time of the process.

Type 3: Those signals could be connected with fast slipping processes during separation of the crack faces at advanced stages of macro-crack opening.

Type 4: This specific type of AE signals also occurs during separation and opening of macro-crack faces and is probably related to interface slipping at fibre pull-out.

4. Conclusions

- Combined measurements of AE and DIC result in information on the crack initiation and propagation as well as the nature of micro-failure mechanisms occurring in distinct regions of the entire fracture process.
- Cracking in UHPC occurs rather localized and brittle without signs of branching cracks.
- An extended FPZ mainly caused by fibre/cement interface failure together with the development of crack branches during macro-crack propagation and the opening of cracks under activation of fibre pull-out processes are reasons for the ductile fracture behaviour of fibre-reinforced UHPC.
- Initiation of cracking and subsequent stages of crack opening and propagation are accompanied by different types of AE signals from different source mechanisms.
- Waveform and frequency analysis of AE signals from located source events in UHPC separates three types of signals that can be correlated with microscopic damage at the transition of the elastic region into the fracture process zone ahead of the macro-crack tip (type 1) and events arising from the stages of propagation and opening of the macro-crack and crack branches as well (type 2 and 3).
- Sources for AE signals of type 4, generated from UHPC/steel fibre material only, are probably related to interface slipping at the process of fibre pull-out.

Acknowledgement

The collaborative investigation between BAM and DTU described in this paper was established with support of BAM in the framework of a research visit of G. Fischer at BAM. The authors would like to acknowledge this support.

References

[1] Shah, S. P. and Carpinteri, A. (1991). Fracture Mechanics Test Methods for Concrete. Chapman and Hall.
[2] Griffith, A. A. (1921). The phenomena of rupture and flow in solids. Philosophical Transactions of the Royal Society of London, 221(1):163-198.
[3] Dugdale, D. S. (1960). Yielding of steel sheets containing slits. Journal of Mechanics and Physics of Solids, 8(1):100_104.
[4] Barenblatt, G. I. (1962). The mathematical theory of equilibrium cracks in brittle fracture. Advances in Applied Mechanics, 7(1):55_129.
[5] Hillerborg, A., Modéer, M., and Petersson, P. E. (1976). Analysis of crack formation and crack growth in concrete by means of fracture mechanics and finite elements. Cement Concrete Research, 6(1):773_782.
[6] Bazant, Z. and Oh, B. (1983). Crack band theory for fracture of concrete. Materials and Structures, 16(93):155_177.
[7] Otsuka, K. and Date, H. (2000). Fracture process zone in concrete tension specimen. Engineering Fracture Mechanics, 65(1):111_131.
[8] Ohno, K, Ohtsu, M: Crack classification in concrete based on acoustic emission. Construction and Building Materials 24 (2010), 2339-2346
[9] Vidya Sagar, R., Prasad, R.V., Rhagu Prasad, B.K., Rao, M.V.S.: Microcracking and Fracture Process in Cement Mortar and Concrete: A Comparative Study Using Acoustic Emission Technique. Experimental Mechanics 53 (2013), 1161-1175
[10] Shahidan, S., Pulin, R., Bunnori, N., Holford, K.M.: Damage classification in reinforced concrete beams by acoustic emission signal analysis. Construction and Building Materials 45 (2013), 78-86
[11] Aggelis, D.G., Mpalaskas, A.C., Ntalakas, D., Matikas, T.E.: Effect of wave distortion on acoustic emission characterization of cementitious materials. Construction and Building Materials 35 (2012), 183-190
[12] Rouchier, S., Foray, G, Godin, N., Woloszyn, M., Roux, J.-J.: Damage monitoring in fibre reinforced mortar by combined digital image correlation and acoustic emission. Construction and Building Materials 38 (2013), 371-380
[13] Fischer, G., Bohse, J.: Observation and Analysis of Fracture Processes in Concrete with Acoustic Emission (AE) and Digital Image Correlation (DIC). 31st Conference of the European Working Group on Acoustic Emission (EWGAE), 3- 5 September 2014, Dresden, Proceedings Th.3.A.4.
[14] Sause, M.G.R., Gribov, A., Unwin, A.R., Horn, S.: Pattern recognition approach to identify natural clusters of acoustic emission signals. Pattern Recognition Letters 33:1 (2012), 17-23
[15] Sause, M.G.R., Horn, S.: Simulation of acoustic emission in planar carbon fiber reinforced plastic specimens. Journal of Nondestructive Evaluation 29:2 (2010), 123-142